Journal of Institute of Science and Technology, 29(2), 83-93 (2024)
ISSN: 2467-9062 (print), e-ISSN: 2467-9240
https://doi.org/10.3126/jist.v29i2.69090

Research Article

GREEN SYNTHESIS OF SILVER NANOPARTICLE USING *Usnea Cornuta* EXTRACT AND ITS APPLICATION ON FORMALDEHYDE SENSING AND ORGANIC DYE DEGRADATION

Amit Lama, Asmita Sapkota, Bindu Gurung, Bishnu Bahadur Sinjali, Krishna Mijar, Nirmala Sharma, Achyut Adhikari*
Central Department of Chemistry, Institute of Science and Technology, Tribhuvan University, Kirtipur, Kathmandu, Nepal
**Correspondence: achyutraj05@gmail.com*

(Received:** August 25, 2024; **Final Revision:** December 20, 2024**; Accepted:** December 22, 2024**)

ABSTRACT

Silver nanoparticles have been widely used in various electronic and sensing devices, coating materials, molecular switches, and data packing. Green synthesis of silver nanoparticles (Ag NPs) has caught much attention in the present world, as it provides an alternative, eco-friendly, and cost-effective process of synthesizing nanoparticles. In this study, Ag NPs were synthesized using *Usnea cornuta* which was further applied for colorimetric sensing of methylene blue (MB) and formaldehyde in water. UV-visible, FTIR, and XRD techniques were used to characterize the synthesized Ag NPs. The formation of Ag NPs was confirmed by a color change and UV-visible spectroscopy which showed the absorption peak at 417 nm. The face-centered cubic (FCC) structure of a crystal with an average size of 8.3 nm was determined by XRD. The presence of polyphenolic groups as capping agents was confirmed by FTIR spectra. Moreover, the synthesized Ag NPs were able to detect methylene blue and formaldehyde solution even in diluted solution i.e. 1 ppm and 1 %, for MB and formaldehyde respectively. Additionally, the AgNps can degrade methylene blue solution. The degradation efficiency of AgNps was found to be 80% at four hours. The *Usnea cornuta* shows good potential as a reducing and stabilizing agent, thus it can be utilized for the biosynthesis of silver nanoparticles. The silver nanoparticle can be utilized to sense organic chemical compounds such as methylene blue and formaldehyde in industrial wastewater as well as other wastes. Thus, Ag NPs show good promising colorimetric sensing abilities.

Keywords: Colorimetric sensing, nanoparticles, *Usnea* spp., UV-visible spectroscopy

INTRODUCTION

Nanotechnology is commonly defined as a scientific field concerned with understanding, controlling, and restructuring nanostructured materials, as well as exploiting materials with fundamentally new properties and functions (Sanchez & Sobolev, 2010). Due to the distinctive physical and chemical properties of nano-scale materials ranging from 1 to 100 nm, their application has increased (Nirmala Grace & Pandian, 2007; Khanal *et al.*, 2022). The two factors, surface effect and quantum effect are primarily responsible for nanomaterial's ability to enhance their properties, including chemical, mechanical, optical, electric, and magnetic (Roduner, 2006). In recent years, metallic nanoparticles (NPs) have been the subject of substantial research, with an interest in applications ranging from catalysts and sensing to optics, antibacterial activity, and data storage (Sudrik *et al.*, 2006). Among various metals, silver nanoparticles (Ag NPs) have been pretty successful in drawing comprehensive attention because of their unique morphologies, stability, and controlled geometry (Nirmala Grace & Pandian, 2007). Ag NPs possess exceptional properties; hence, they are applied in various fields: biomedical, drug delivery, water treatment, agriculture, ink, adhesives, pastes, and much more (Chaloupka *et al.*, 2010; Dankovich & Gray, 2011; Nair *et al.*, 2010; Park *et al.*, 2018; Prow *et al.*, 2011).

Furthermore, Ag NPs are easy to synthesize, low-cost, and versatile materials. Like other noble metal nanoparticles, the colorimetric sensing application of Ag NPs also depends upon the quantitative coupling of silver nanoparticles, which results from a significant change in the photonic properties through aggregation mechanisms that ultimately lead to a change in color. For these reasons, the Ag NPs have a promising future as visual colorimetric sensors for the identification of target materials (Laliwala *et al.*, 2014; Kumar *et al.*, 2014). Significantly, the Ag NPs show very high extinction coefficients, and the plasmonic band of Ag NPs can be varied depending on their size and distance, making them potential naked-eye distinctive readout sensors (Vilela *et al.*, 2012; Kailasa *et al.*, 2018).

The Green synthesis method has been drawing attention these days because of its environment-friendly nature and biocompatibility which includes plant extracts, bacteria, actinomycetes, fungi, and enzymes for the synthesis of Ag NPs (Husen, 2017; Husen & Siddiqi, 2014; Subba Rao *et al.*, 2013; Tagad *et al.*, 2013; Venkateswarlu *et al.*, 2015).

Lichens are a composite organism consisting of a fungus and green algae that function in a symbiotic relationship or association (Mie *et al.*, 2014). *Usnea* is a genus of

usually pale grayish-green fruticose lichens that develop in the form of leafless mini-shrubs or tassels anchored on bark or twigs. It belongs to the family Parmeliaceae. It is cosmopolitan in distribution. Members of the genus are sometimes known as old man's beard or beard lichen (Sharnoff & Rave, 2014). Additionally, lichens also possess several varieties of metabolites, such as polysaccharide (homo-D-glucan) and phenolic (depside, depsidon, and dibenzofuran) compounds, which have the potential to act as reducing and capping agents for silver ions (Culberson, 1979; Elix *et al.*, 1984). The lichens of genus *Usnea* have been reported to contain several compounds such as usnic acid, usenamines, usone, iso-usones, mono-substituted phenyls, anthraquinones, dibenzofurans, terpenoids, etc., which may be responsible for the synthesis of Ag NPs (Fernández-Moriano *et al.*, 2016; Halici *et al.*, 2005; Nishitoba *et al.*, 1987; Yu *et al.*, 2016).

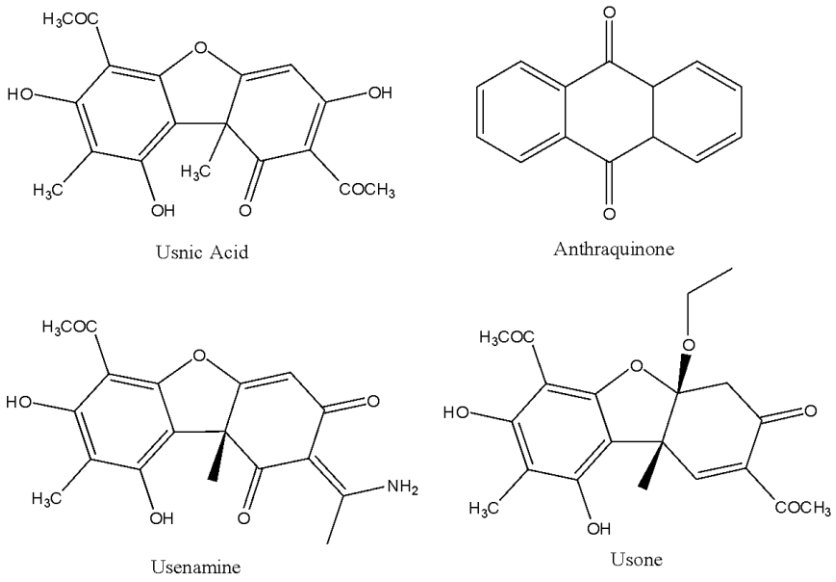

Figure 1. Secondary metabolites isolated from *Usnea* spp.

Silver nanoparticles display specific optical characteristics in the visible region (380–750 nm), thus attracting attention for their application in chemical or biochemical sensing systems and optoelectronic devices. When the nanoparticles (NPs) are smaller than the incident light wavelength, and the surface plasmon is confined near such nanoparticles, localized surface plasmon resonance (LSPR) has resulted. The frequency and intensity of such LSPR absorption bands rely on the type, shape, size, and size distribution of nanoparticles, offering a broad variety of sensing applications (Zarger & Hatamie, 2013; Austin *et al.*, 2014; Nehl & Hafner, 2014; Amirjani *et al.*, 2016a; Amirjani *et al.*, 2016b). Furthermore, the characteristics of Ag NPs that are most frequently used in sensing applications are dependent on variations in the dielectric constant of the surrounding medium, which can occur through complex formation at the nanoparticle surface or by altering the solvent quality. Several investigations have demonstrated that LSPR shifts towards a higher wavelength in the presence of a less polar medium (Kreibig & Vollmer, 1995; Link & El-Sayed, 2000).

The main reasons for the colorimetric change of Ag NPs are particle surface modification and aggregation. In most cases, interparticle bond formation (cross-linking aggregation) or changes to colloidal stability (non-cross-linking aggregation) cause nanoparticles to aggregate (Zhao, 2008). The optical absorbance is greatly altered by both surface plasmon coupling and distance in nanoparticles, leading to the detection of target molecules. The NPs aggregate as a result of interactions between the target analytes and NPs, which can take the form of hydrogen bonds or electrostatic interactions. Furthermore, the kind and quantity of the analytes affect the level of NP aggregation, which is demonstrated by a color shift; a UV-visible spectrophotometer measures the absorption band (Qin *et al.*, 2018). This property of NP can be beneficial for the detection of harmful chemicals like formaldehyde. Previous techniques include UV-vis spectroscopy, HPLC, paper-kit, GCMS, and other spectrophotometry techniques. While these methods can produce great sensitivity and accuracy, each methodology still has some limitations. The main purpose of this study was to carry out the green synthesis of Ag NPs using *Usnea* spp., characterize it, and its application as a colorimetric sensor against formalin. This could be an easy-to-handle and quick method for sensing chemicals like formalin in the context of Nepal. Another goal of this research is to study the catalytic degradation of organic dye by silver nanoparticles.

MATERIALS AND METHODS

Chemicals

During the research project, the following chemicals were used: formaldehyde (Fisher Scientific), sodium hydroxide (Fisher Scientific), distilled water, Whatman filter paper 1, ammonia (Merck), methylene blue (Merck), and silver nitrate (Merck). All of the chemicals were of analytical grades.

Collection and Identification of Plant

A fresh lichen species *Usnea cornuta* sample was collected from Daman, Makwanpur. The sample was collected based on the ethnobotanical ideas of local people and a literature review. The lichen samples were identified from the Central Department of Botany, Tribhuvan University, Nepal. After being cleaned with sterile, double-distilled water, the samples were allowed to air dry. It was ground into a coarse powder using a mechanical grinder. The powder was gathered and kept dry and refrigerated until it was needed for more research.

Plant Extract Preparation

Initially, 150 mL of distilled water and 3 g of lichen powder were brought to a boil for 30 minutes at 60 °C. The mixture was then allowed to cool. Following that, Whatman No. 1 filter paper was used twice to filter it. The resulting filtrate, referred to as the plant extract, was collected and put aside for further study, while the remaining plant residue was refrigerated at 4 °C.

Green Synthesis of Silver Nanoparticles

In a conical flask, 10 mL of lichen extract was first added, and after 30 minutes of continuous stirring, 50 mL of a 1 mM $AgNO_3$ solution was added at room temperature. The pH of the solution was maintained at 10 using 0.1 M HCl and 0.1 mM NaOH solution. The presence of a UV peak maximum at 417 nm in UV spectra, together with a color shift from yellow to a dark reddish color, validated the synthesis of Ag NPs. Following synthesis, the Ag NPs were isolated and purified.

Characterization of Ag NPs

The synthesis, size, crystallinity, form, and amount of the created Ag NPs were all examined. UV-visible spectroscopy and X-ray diffraction were the two main methods used to characterize the produced Ag NPs.

UV-Visible Absorbance Spectroscopy

The process of verifying the creation of Ag NPs involved recording UV spectra and analyzing the absorption band and bandgap using the SPECORD 200 PLUS, analytikjena (An Endress+Hauser Company) UV-visible spectrophotometer. The samples were scanned at a medium scanning rate with a 1 nm resolution in the 300–700 nm range. In the experiment, the baseline correction of the spectrophotometer was set using distilled water as a benchmark. Each sample was placed in a quartz cuvette that held 2 mL and had a route length of 1 cm.

X-Ray Diffraction

The XRD method was used to characterize the crystallinity and structure of the produced Ag NPs. Using mono-chromated Cu Kα radiation with a wavelength of 1.54060 Å, the Rigaku D/MAX-2500/pc diffractometer was used to record the routine powder X-ray diffraction patterns for the specified dried Ag NPs. The scan rate was 10°/minute throughout the 2θ angle, which ranged from 0 to 90, with 30 mA current and 40 kV voltage.

Fourier Transforms Infrared Spectroscopy (FTIR)

FTIR is a valuable instrument for detecting the presence of functional groups since individual bonds frequently have distinct energy absorption bands. FTIR analysis was used to characterize the presence of organic groups that might be involved in the synthesis of Ag NPs. Furthermore, Ag NPs' surface can be used by FTIR to determine whether organic functional groups are present. The scan range for the spectra was 4000–400 cm^{-1}.

Detection of Chemical Compounds

The synthesized Ag NPs were used for the detection of different kinds of chemical compounds including ammonia, p-nitrophenol, formaldehyde, nitrobenzene, and aminophenol. Firstly, tested sample solutions of varying concentrations: 30%, 20%, 10%, and 1% were prepared. 2 mg/mL concentration of Ag-NPs was taken and then about 0.5 mL of synthesized Ag NPs solution was mixed into each test tube. The color change was observed, and photographic images were captured. In addition, the resulting solution mixture was subjected to a UV-visible spectrophotometer.

Catalytic Degradation of Organic Dye

Green-synthesized silver nanoparticles were employed as catalysts for the degradation of the organic dye methylene blue, followed by the addition of H_2O_2. Methylene blue is an aromatic chemical compound with a heterocyclic structure and the molecular formula $C_{16}H_{18}C_lN_3S$. For the catalytic degradation of methylene blue stock solution, concentrations of 10 ppm were prepared. The catalytic degradation was carried out with a green-synthesized silver nanoparticle colloidal solution in a 2 mL quartz cuvette with a path length of 1 cm. To track the progress of the reactions, the absorbance was measured for kinetic studies using a UV-visible spectrophotometer at various time intervals, starting at 0 minutes, 30 minutes, 1 hour, 1 hour 30 minutes, 2 hours, 2 hours 30 minutes, 3 hours, 3 hours 30 minutes, and finishing at 4 hours. Thus, progress of the reaction of the resulting solution was carried out then taking the absorbance maxima at various time intervals, the degradation efficiency was estimated.

$$\text{Efficiency} = (A_o - A) / A_o$$

Efficiency is defined as the ratio of difference in concentration (A_0-A) to initial concentration (A_o). It is estimated in percentage. In which, efficiency (%)

represents the degradation efficiency of dye,
A_o = absorbance of dye solution at zero time,
A= absorbance of dye solution in suspension after time t.

RESULT AND DISCUSSIONS

Green Synthesis of Ag NPs

Aqueous lichen extracts were used to create the silver nanoparticles. The synthesis of Ag NPs was tentatively confirmed by the color shift from orange to dark brownish red. The solution's apparent color shift most closely matched Dasari's earlier research in the literature (Dasari *et al.*, 2013). The visual read-out color change can be observed through the photographic images of lichen extract solutions and Ag NPs, as shown in **Figure 2**. In contrast, the solution after one hour looked browner, as did the solution after twenty-four hours. Ag NPs' size-dependent quantum confinement characteristics, which also impact their optical qualities, are responsible for this hue shift. The presence of Ag NPs was indicated by the dark brownish-red hue of the solutions after 24 hours and 1 hour, with an increase in absorbance from 0.9893 to 2.466. Additionally, as the incubation duration grew, the brown color's intensity rose as a result of the reduction of $AgNO_3$ and the activation of the surface plasmon resonance (SPR) effect (Krishnaraj *et al.*, 2010). The $AgNO_3$ solution was transparent and clear in contrast to the Ag NPs solutions, whereas the lichen extract solution was only orange.

UV-Visible spectrophotometer:

The characterization of thus prepared Ag NPs was carried out using a UV-visible spectrophotometer. The UV-visible spectra of the lichen extract are shown in Figure 3.

Figure 2. Photographic images of lichen Extract (left) and silver nanoparticles (right)

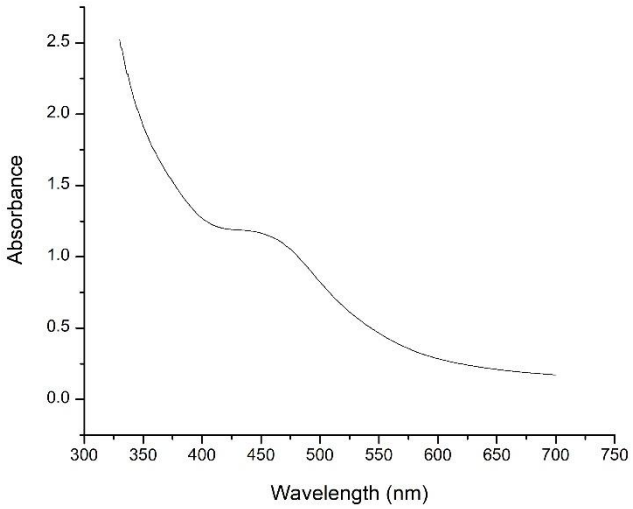

Figure 3. UV spectra of *Usnea* spp. extract

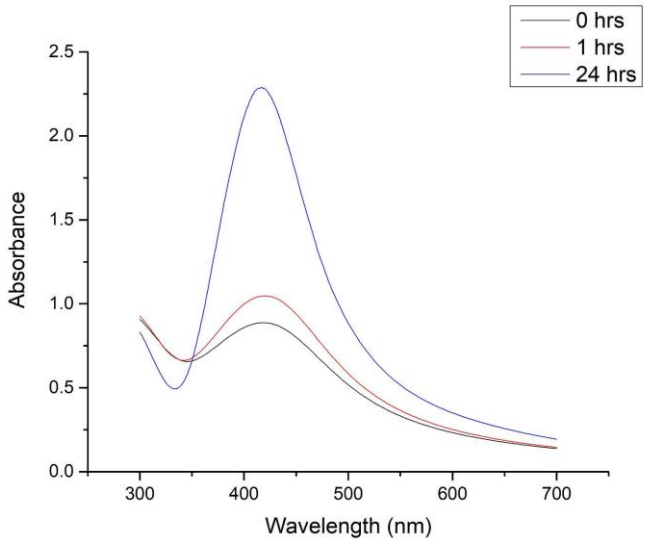

Figure 4. UV spectra of biosynthesized silver nanoparticles in different time intervals.

Contrarily, the UV-visible spectra (Figure 4) of synthesized Ag NPs show absorption peaks at 422 nm, 421 nm, and 417 nm in 0 hr, 1 hr, and 24 hr, respectively, which espoused confirmation for the formation of silver nanoparticles (Dasari *et al.*, 2013). Previous research has shown that AgNPs have SPR peaks in the 400–450 nm wavelength region, and this finding was in good accord with the studied results. Various functional groups present in lichen extracts can bind silver, which facilitates the formation of small-sized nanoparticles. The appearance of absorption peaks in the UV-visible spectra was caused by the SPR phenomenon. The so-called surface plasmon resonance (SPR) phenomenon was caused by electromagnetic radiation stimulating the surface plasmon that was present on the Ag NPs' outer surface. Furthermore, the produced nanoparticles' size, shape, content, and dielectric characteristics affect the SPR bands (Kelly *et al.*, 2003).

X-ray Diffraction (XRD)

XRD analysis was used to confirm the crystalline structure of the Ag NPs that were biosynthesized using an aqueous extract of *Usnea* spp. The XRD pattern of the dried Ag NPs is shown in Figure 5.

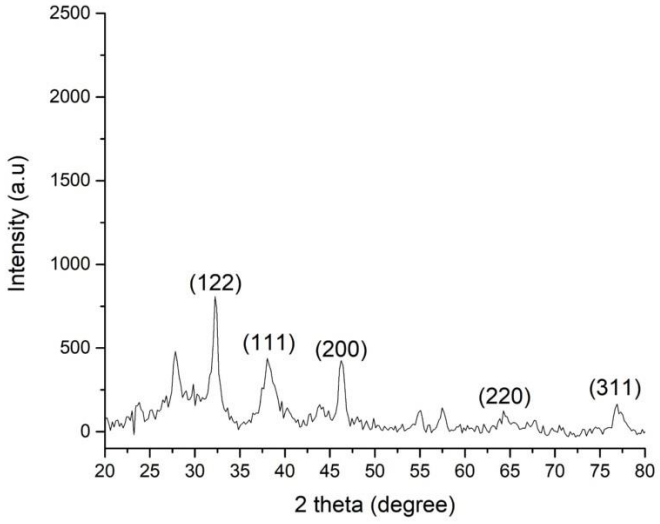

Figure 5. XRD diffraction pattern of silver nanoparticles

Four separate peaks can be seen in Figure 5 for 2θ values of 38.20°, 46.27°, 64.40°, and 77.09°, respectively. The corresponding lattice plane values are (111), (200), (220), and (311). Additionally, every one of these diffraction peaks matches the features of the metallic face-centered cubic (FCC) silver phase, which is consistent with the standard JCPDS Card number 04-0783 database. Thus, this demonstrates that the artificially produced silver nanoparticles are crystalline (Din *et al.*, 2015). In addition to this, these values are consistent with the previously

reported results (Mie *et al.*, 2014; Cruz *et al.*, 2010; Mohammad, 2010; Jain *et al.*, 2009). In addition, the crystalline nature of the bio-organic phase (capping agent) on the surface of Ag NPs could be the cause of other distinctive peaks. The partial oxidation of silver may also cause these characteristic peaks to appear in the silver oxide (Anandalakshmi *et al.*, 2016). Based on the width of all diffraction peaks obtained by the Gaussian fitting of all three peaks using Debye-Scherrer's formula, the average crystalline size of the biosynthesized Ag NPs was found to be 8.3 nm (Anandalakshmi *et al.*, 2016).

Fourier Transforms Infrared Spectroscopy (FTIR)

Both lichen extract and the synthesized Ag NPs were subjected to FTIR analysis, and the results are represented in Figure 6.

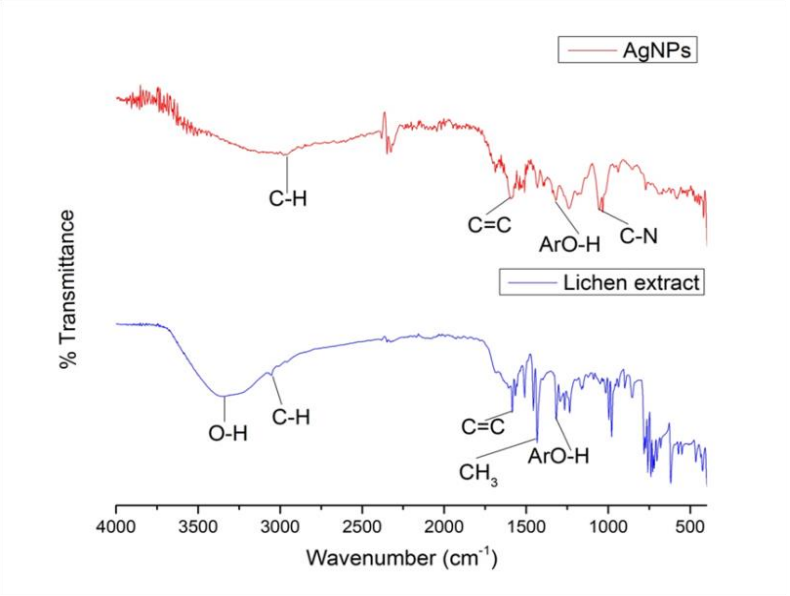

Figure 6. FTIR of lichen extract and biosynthesized Ag NP

The presence of functional groups in the material can be inferred from FTIR spectra. The absorption peaks at 2957, 1598, 1319, and 1053 cm^{-1} were discovered to be indicative of the existence of aromatic C-H stretching, aromatic C=C stretching, aromatic O-H stretching, and amine-containing C-N stretching, respectively. Similar absorption peaks were seen in the FTIR spectra of the lichen extract at 3339, 3050, 1585, 1433, and 1316 cm^{-1}, which corresponded to the O-H stretching (H-bonded), aromatic C-H stretching, C=C stretching, methyl group, and aromatic O-H stretching (phenolic O-H), respectively (Anandalakshmi *et al.*, 2016; Jeeva *et al.*, 2014). The FTIR spectra show the oxidized phenolic groups acting as the capping agents.

Application of Ag NPs in Detection of Formaldehyde

The synthesized Ag NPs solution was applied in sensing different organic compounds such as formaldehyde, nitrobenzene, ammonia, nitrophenol, and aminophenol. However, the Ag NPs solution was capable of detecting only formaldehyde.

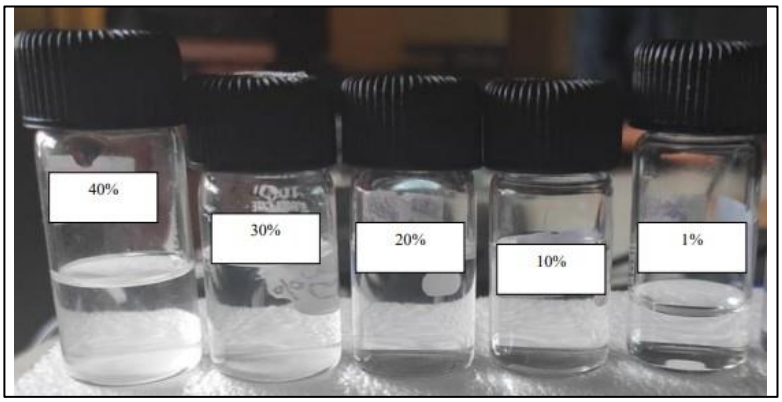

Figure 7a. Photographic image of formaldehyde solutions of different concentrations

Figures 7a and 7b display the photographic pictures of formaldehyde alone and with Ag NPs added. The photos demonstrate how the addition of Ag NPs solution changed the formaldehyde's color. Figure 7a illustrates how colorless the formaldehyde solutions are before the addition of the Ag NPs solution. In a matter of seconds, after the Ag NPs solution was added, the 40% formaldehyde solution started to turn a dark red color. In a similar vein, the formaldehyde solution at 30% looked black, the solution at 20% looked pale reddish black, the solution at 10% looked red, and the solution at 1% looked yellowish. But after three to five minutes, these solutions' colors started to shift even more. The 40% and 30% formaldehyde solutions further changed to black color. The 20% formaldehyde solution further changed to reddish black.

When 10% formaldehyde was added, the hue further altered to a blackish crimson. 1% formaldehyde underwent a color shift, appearing yellowish-red. The observed alteration in hue can be ascribed to the alteration in the linear surface tension ratio (LSPR) of silver nanoparticles (Ag NPs), which arises from the interplay between electrons on their surface and electromagnetic radiation (Prosposito *et al.*, 2020).

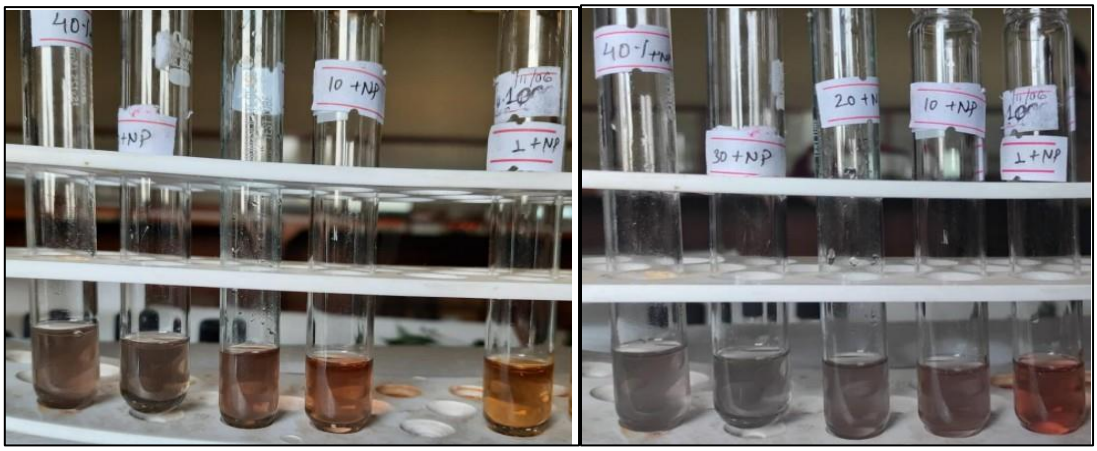

Figure 7b. Photographic images showing color change of formaldehyde solutions of different concentrations after the addition of Ag NPs solution

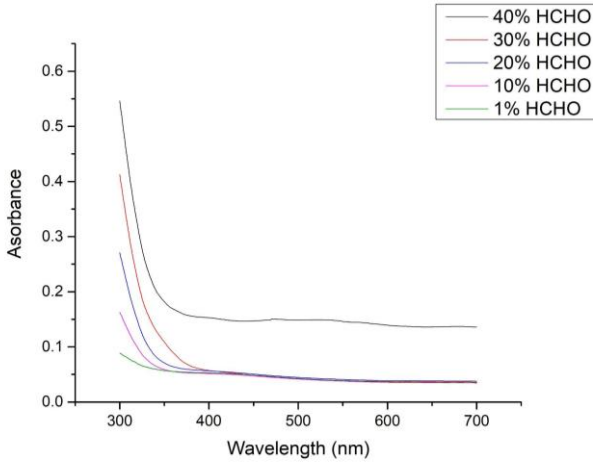

Figure 8a. UV spectra of formaldehyde solutions of different concentrations

With a UV-visible spectrometer, the resultant solution mixture was further examined by looking for changes in the absorbance band.

The UV absorbance spectra of a formaldehyde solution at different concentrations are displayed in Figure 8a. It is evident from the figure that none of the formaldehyde solutions exhibit a discernible absorbance peak in the 400–450 nm range. As seen in Figure 8b, strong absorbance peaks were seen at 411-416 nm upon the addition of Ag NPs. A progressive change in the spectrum maximum can be seen in Figure 8b if compared with the silver nanoparticles. Additional broad peaks are formed towards higher wavelengths. Redshift was also observed in previous research. Furthermore, the absorption peak strength

often rises as the formaldehyde solution is diluted. This could be because the diluted formaldehyde solution contains more free Ag NPs. The concentrated formaldehyde solution and the Ag NPs mixed solution, on the other hand, had a lower concentration of free Ag NPs because of Ag NP buildup. The interaction between Ag NPs and formaldehyde solution is responsible for the spectral and color changes of the solution that were observed (Qin *et al.*, 2018). Though synthesized silver nanoparticles can detect formaldehyde in some amount, it has a poor sensitivity. It could not sense formaldehyde below 2.6 mgL^{-1}, which is a tolerable concentration limit recommended by the World Health Organization.

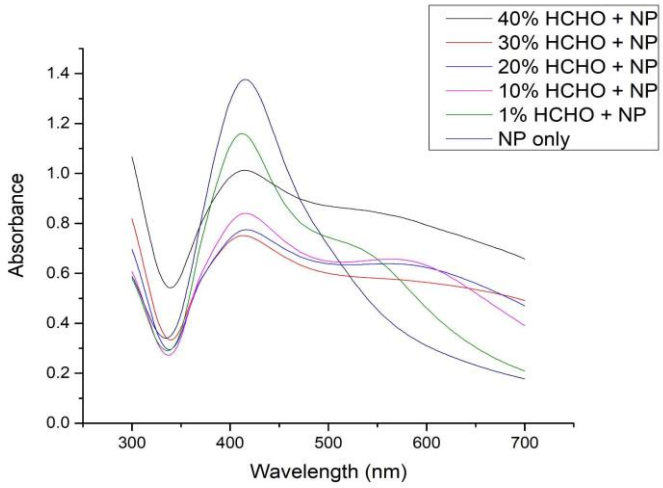

Figure 8b. UV spectra of different concentration of formaldehyde after addition of Ag NPs solution.

Application of Ag NPs in Catalytic Degradation of Organic Dye

To assess the catalytic performance of Ag NPs, the catalytic degradation of methylene blue was conducted at different time intervals in the visible spectrum (as shown in Figure 9). When Ag NPs were introduced as a catalyst, the absorption spectrum revealed diminishing peaks for methylene blue. The gradual reduction in methylene blue's absorbance values, approaching the baseline, indicated the progressive degradation of methylene blue. Eventually, the methylene blue peak disappeared entirely as the reaction time increased, signifying the successful degradation of methylene blue.

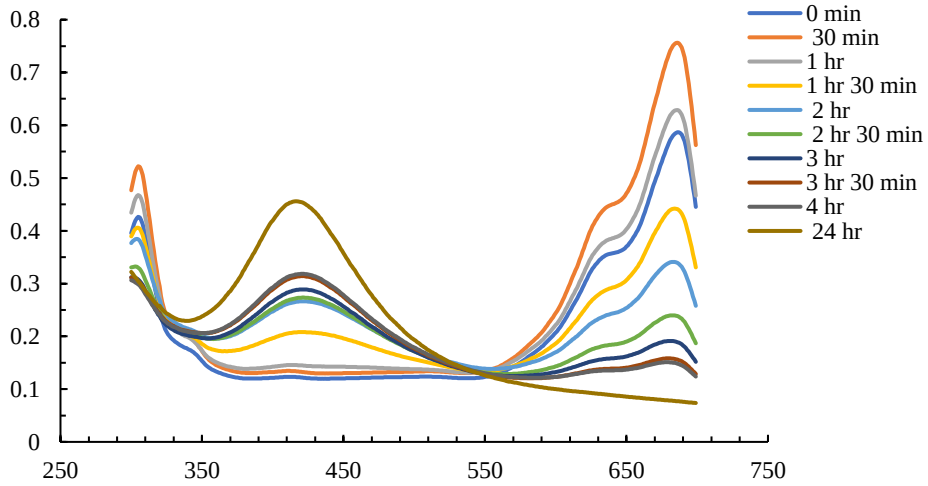

Figure 9. UV-visible spectra of the degradation of Methylene Blue with the assistance of silver nanoparticles as a catalyst.

In this process of dye degradation, the maximum absorption of the methylene blue was at 0.7761 at the initial concentration. After 30 min, maximum absorption was observed at 0.7558 and efficiency was estimated which was found to be 2.62 %. Then at each interval of time, efficiency was increased. Eventually, after four hours, the maximum absorption of the methylene blue on the UV spectrum was recorded at 0.1509 then, efficiency was calculated, and it was found to be 80%. The result shows that AgNPs can play a

crucial role in degrading MB in the presence of sunlight and the efficiency, of degrading MB solution, increases gradually with the increase in time of exposure to sunlight. It is owing to π ⟶ π∗ and n⟶ π∗ transitions and shifting of lambda max value by sun rays which assist in decolorizing the MB solution.

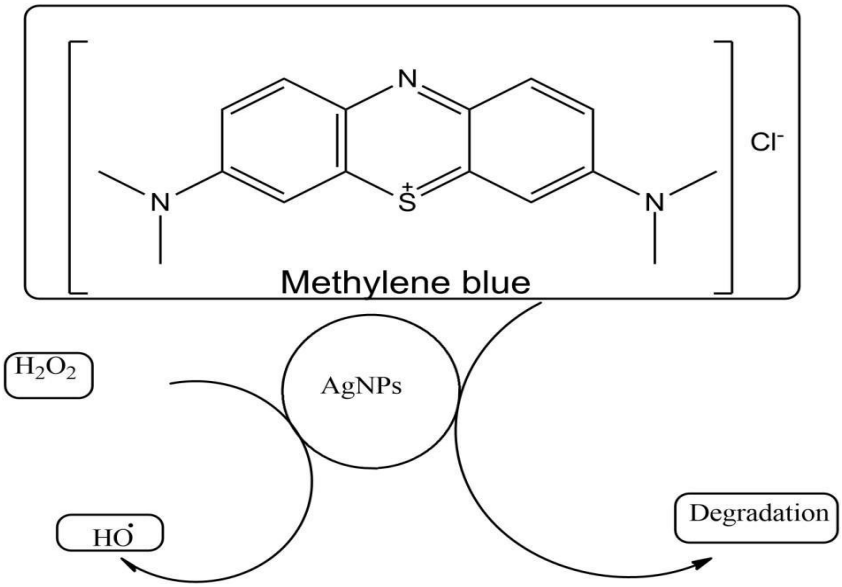

Figure 10. Sketch of degradation of Methylene blue

Ag NPs' greater surface area contributes to their degrading characteristic. A study on the catalytic degradation characteristics of silver nanoparticles made from *P. ovata* leaf extract was previously carried out by Githala *et al.* (2022). They claimed that the reaction was finished in 20 minutes and that Methylene Blue's color was eliminated. According to these findings, silver nanoparticles made from *P. ovata* leaf extract demonstrated potent catalytic capabilities in the Methylene Blue breakdown process (Githala *et al.*, 2022). Furthermore, Jyoti *et al.* (2016) looked into the catalytic activity of Ag NPs in the reduction of the water pollutant methylene blue. As the dye's absorbance value declined and the amount of silver nanoparticles increased, the absorption peaks revealed fewer peaks with time. As response times increased, Methylene Blue dye began to degrade (Jyoti & Singh, 2016). These previous results align perfectly with current research on the catalytic degradation activity of Ag NPs against the organic dye methylene blue.

CONCLUSIONS

Silver nanoparticles synthesized from the extract of *Usnea cornuta* were found to be effective for the colorimetric sensing of formaldehyde in an aqueous solution. Furthermore, methylene blue, an organic dye, was catalytically degraded by silver nanoparticles.

ACKNOWLEDGMENTS

We would like to thank Associate Professor Dr. Chitra Bahadur Baniya for Lichen identification.

ABBREVIATIONS

SPR: Surface Plasmon Resonance; LSPR: localized surface plasmon resonance; NPs: Nanoparticles; AgNPs: silver nanoparticles; MB: Methylene Blue; FCC: Face Centered Cube; XRD: X-Ray Diffraction.

AUTHOR CONTRIBUTIONS

AA supervised the research work and contributed to the conception and design of the study. AL carried out the laboratory works and data analysis. AL and BG interpret the results. AS, BBS, KM and NS drafted the manuscript. All authors reviewed the results and approved the final version of the manuscript.

CONFLICTS OF INTEREST

The authors declare no conflicts of interest.

DATA AVAILABILITY

All the data collected throughout the course of this study has been comprehensively presented and visually represented within the manuscript.

REFERENCES

Amirjani, A., Bagheri, M. Heydari, M., & Hesaraki, S. (2016b). Label-free surface plasmon resonance detection of hydrogen peroxide; a bio-inspired approach. *Sensors and Actuators B: Chemical*, 227, 373-382.

Amirjani, A., Bagheri, M., Heydari, M., & Hesaraki, S. (2016a). Colorimetric determination of Timolol concentration based on localized surface plasmon resonance of silver nanoparticles. *Nanotechnology*, 27(37), 375503.

Anandalakshmi, K., Venugobal, J., & Ramasamy, V. (2016). Characterization of silver nanoparticles by green synthesis method using *Pedalium murex* leaf

extract and their antibacterial activity. *Applied Nanoscience*, 6(3), 399–408.

Austin, L.A., Mackey, M.A., Dreaden, E.C., & El-Sayed, M.A. (2014). The optical, photothermal, and facile surface chemical properties of gold and silver nanoparticles in biodiagnostics, therapy, and drug delivery. *Archives of Toxicology*, 88(7), 1391–1417.

Chaloupka, K., Malam, Y., & Seifalian, A.M. (2010). Nanosilver as a new generation of nanoproduct in biomedical applications. *Trends in Biotechnology,* 28(11), 580–588.

Cruz, D., Falé, P.L., Mourato, A., Vaz, P.D., Serralheiro, M.L., & Lino, A.R.L. (2010). Preparation and physicochemical characterization of Ag nanoparticles biosynthesized by *Lippia citriodora* (Lemon Verbena). *Colloids and Surfaces B: Biointerfaces*, 81(1), 67–73.

Culberson, C.F. (1979). *Chemical and Botanical Guide to Lichen Products*. Otto Koeltz Science Publishers.

Dankovich, T.A., & Gray, D.G. (2011). Bactericidal paper impregnated with silver nanoparticles for point-of-use water treatment. *Environmental Science & Technology*, 45(5), 1992–1998.

Dasari, S., Suresh, K.A., Rajesh, M., Reddy, C.S.S., Hemalatha, C.S., Wudayagiri, R., & Valluru, L. (2013). Biosynthesis, characterization, antibacterial and antioxidant activity of silver nanoparticles produced by lichens. *Journal of Bionanoscience*, 7, 237–244.

Din, L.B., Mie, R., Samsudin, M.W., Ahmad, A., & Ibrahim, N. (2015). Biomimetic synthesis of silver nanoparticles using the lichen *Ramalina dumeticola* and the antibacterial activity. *Malaysian Journal of Analytical Sciences*, 19(2), 369-376.

Elix, J.A., Whitton, A.A., & Sargent, M.V. (1984). Recent progress in the chemistry of lichen substances (pp. 103–234). In Herz, W., Grisebach, H., & Kirby, G.W. (Eds.), *Fortschritte der Chemie organischer Naturstoffe / Progress in the Chemistry of Organic Natural Products*, Vienna: Springer.

Fernández-Moriano, C., Gómez-Serranillos, M.P., & Crespo, A. (2016). Antioxidant potential of lichen species and their secondary metabolites. A systematic review. *Pharmaceutical Biology*, 54, 1–17.

Githala, C.K., Raj, S., Dhaka, A., Mali, S.C., & Trivedi, R. (2022). Phyto-fabrication of silver nanoparticles and their catalytic dye degradation and antifungal efficacy. *Frontiers in Chemistry*, 10. https://doi.org/10.3389/fchem.2022.994721.

Grace, A.N., & Pandian, K. (2007). Antibacterial efficacy of aminoglycosidic antibiotics protected gold nanoparticles—A brief study. *Colloids and Surfaces A: Physicochemical and Engineering Aspects*, 297(1), 63–70.

Halici, M., Odabasoglu, F., Suleyman, H., Cakir, A., Aslan, A., & Bayir, Y. (2005). Effects of water extract of *Usnea longissima* on antioxidant enzyme activity and mucosal damage caused by indomethacin in rats. *Phytomedicine*, 12, 656–662.

Husen, A., & Siddiqi, K.S. (2014). Phytosynthesis of nanoparticles: concept, controversy and application. *Nanoscale Research Letters*, 9, 229.

Husen, A., (2017). Gold nanoparticles from plant system: synthesis, characterization and their application (pp. 455–479). In Ghorbanpour, M., Manika, K., & Varma, A. (Eds.), *Nanoscience and Plant–Soil Systems*. Cham: Springer International Publishing.

Jain, D., Daima, H., Kachhwala, S., & Kothari, S. (2009). Synthesis of plant-mediated silver nanoparticles using papaya fruit extract and evaluation of their anti-microbial activities. *Digest Journal of Nanomaterials and Biostructures*, 4, 557–563.

Jeeva, K., Thiyagarajan, M., Elangovan, V., Geetha, N., & Venkatachalam, P. (2014). *Caesalpinia coriaria* leaf extracts mediated biosynthesis of metallic silver nanoparticles and their antibacterial activity against clinically isolated pathogens. *Industrial Crops and Products*, 52, 714–720.

Jyoti, K., & Singh, A., (2016). Green synthesis of nanostructured silver particles and their catalytic application in dye degradation. *Journal of Genetic Engineering and Biotechnology*, 14(2), 311–317.

Kailasa, S.K., Koduru, J.R., Desai, M.L., Park, T.J., Singhal, R.K., & Basu, H. (2018). Recent progress on surface chemistry of plasmonic metal nanoparticles for colorimetric assay of drugs in pharmaceutical and biological samples. *TrAC Trends in Analytical Chemistry,* 105, 106–120.

Kelly, K.L., Coronado, E., Zhao, L.L., & Schatz, G.C. (2003). The optical properties of metal nanoparticles: The influence of size, shape, and dielectric environment. *The Journal of Physical Chemistry B*, 107(3), 668–677.

Khanal, L.N., Sharma, K.R., Paudyal, H., Parajuli, K., Dahal, B., Ganga, G.C., Pokharel, Y.R., & Kalauni, S.K. (2022). Green synthesis of silver nanoparticles from root extracts of *Rubus ellipticus* Sm. and comparison of antioxidant and antibacterial activity. *Journal of Nanomaterials*, e1832587. https://doi.org/10.1155/2022/1832587.

Kreibig, U., & Vollmer, M. (Eds.) (1995). *Optical properties of metal clusters*. Springer Series on Materials Science 25, Springer.

Krishnaraj, C., Jagan, E.G., Rajasekar, S., Selvakumar, P., Kalaichelvan, P.T., & Mohan, N. (2010). Synthesis of silver nanoparticles using *Acalypha indica* leaf extracts and its antibacterial activity against water borne pathogens. *Colloids and Surfaces B: Biointerfaces*, 76(1), 50–56.

Kumar, V.V., Anbarasan, S., Christena, L.R., SaiSubramanian, N., & Anthony, S.P. (2014). Bio-functionalized silver nanoparticles for selective colorimetric sensing of toxic metal ions and antimicrobial studies. *Spectrochimica Acta Part A: Molecular and Biomolecular Spectroscopy*, 129, 35–42.

Laliwala, S.K., Mehta, V.N., Rohit, J.V., & Kailasa, S.K. (2014). Citrate-modified silver nanoparticles as a colorimetric probe for simultaneous detection of four triptan-family drugs. *Sensors and Actuators B: Chemical*, 197, 254–263.

Link, S., & El-Sayed, M.A. (2000). Shape and size dependence of radiative, non-radiative and photothermal properties of gold nanocrystals. *International Reviews in Physical Chemistry*, 19(3), 409–

453.

Mie, R., Samsudin, M.W., Din, L.B., Ahmad, A., Ibrahim, N., & Adnan, S.N.A. (2014). Synthesis of silver nanoparticles with antibacterial activity using the lichen *Parmotrema praesorediosum*. *International Journal of Nanomedicine*, 9(1), 121–127.

Mohammad, G. (2010). Biosynthesis of silver nanoparticles using plant extracts. *Journal of Biological Sciences*, 10(5), 465-467.

Nair, R., Varghese, S.H., Nair, B.G., Maekawa, T., Yoshida, Y., & Kumar, D.S. (2010). Nanoparticulate material delivery to plants. *Plant Science*, 179(3), 154–163.

Nehl, C.L., & Hafner, J.H. (2008). Shape-dependent plasmon resonances of gold nanoparticles. *Journal of Materials Chemistry*, 18(21), 2415–2419.

Nishitoba, Y., Nishimura, I., Nishiyama, T., & Mizutani, J. (1987). Lichen acids, plant growth inhibitors from *Usnea longissimi*. *Phytochemistry*, 26(12), 3181–3185.

Park, K., Seo, D., & Lee, J. (2008). Conductivity of silver paste prepared from nanoparticles. *Colloids and Surfaces A: Physicochemical and Engineering Aspects*, 313–314, 351–354.

Prosposito, P., Burratti, L., & Venditti, I. (2020). Silver nanoparticles as colorimetric sensors for water pollutants. *Chemosensors*, 8(2), 26.

Prow, T.W., Grice, J.E., Lin, L.L., Faye, R., Butler, M., Becker, W., Wurm, E.M.T., Yoong, C., Robertson, T.A., Soyer, H.P., & Roberts, M.S. (2011). Nanoparticles and microparticles for skin drug delivery. *Advanced Drug Delivery Reviews*, 63(6), 470–491.

Qin, L., Zeng, G., Lai, C., Huang, D., Xu, P., hang, C., Cheng, M., Liu, X., Liu, S., Li, B., & Yi, H. (2018). Gold rush' in modern science: Fabrication strategies and typical advanced applications of gold nanoparticles in sensing. *Coordination Chemistry Reviews*, 359, 1–31.

Roduner, E. (2006). Size matters: why nanomaterials are different. *Chemical Society Reviews*, 35, 583-592. https://doi.org/10.1039/B502142C.

Sanchez, F., & Sobolev, K. (2010). Nanotechnology in concrete – A review. *Construction and Building Materials*, 24(11), 2060–2071.

Sharnoff, S., & Raven, P.H. (1979). *A Field Guide to California Lichens*, Illustrated edition. Yale University Press.

Subba Rao, Y., Kotakadi, V. S., Prasad, T.N.V.K.V., Reddy, A.V., & Sai Gopal, D.V.R. (2013). Green synthesis and spectral characterization of silver nanoparticles from Lakshmi Tulasi (*Ocimum sanctum*) leaf extract. *Spectrochimica Acta Part A. Molecular and Biomolecular Spectroscopy*, 103, 156–159.

Sudrik, S.G., Chaki, N.K., Chavan, V.B., Chavan, S.P., Chavan, S.P., Sonawane, H.R., & Vijayamohanan, K. (2006). Silver nanocluster redox-couple-promoted nonclassical electron transfer: an efficient electrochemical wolff rearrangement of α-diazoketones. *Chemistry – European Journal,* 12(3), 859–864.

Tagad, C.K., Dugasani, S.R., Aiyer, R., Park, S., Kulkarni, A., & Sabharwal, S. (2013). Green synthesis of silver nanoparticles and their application for the development of optical fiber based hydrogen peroxide sensor. *Sensors and Actuators B: Chemical*, 183, 144–149.

Venkateswarlu, S., Kumar, B.N., Prathima, B., Anitha, K., & Jyothi, N.V.V. (2015). A novel green synthesis of Fe_3O_4-Ag core shell recyclable nanoparticles using *Vitis vinifera* stem extract and its enhanced antibacterial performance. *Physica B: Condensed Matter*, 457, 30–35.

Vilela, D., González, M.C., & Escarpa, A. (2012). Sensing colorimetric approaches based on gold and silver nanoparticles aggregation: Chemical creativity behind the assay. A review. *Analytica Chimica Acta*, 751, 24–43.

Yu, X., Guo, Q., Su, G., Yang, A., Hu, Z., Qu, C., Wan, Z., Li, R., Tu, P., & Chi, X. (2016). Usnic acid derivatives with cytotoxic and antifungal activities from the lichen *Usnea longissimi*. *Journal of Natural Products*, 79(5), 1373–1380.

Zargar, B., & Hatamie, A. (2013). Localized surface plasmon resonance of gold nanoparticles as colorimetric probes for determination of Isoniazid in pharmacological formulation. *Spectrochimica Acta Part A: Molecular and Biomolecular Spectroscopy*, 106, 185–189.

Zhao, W. (2008). *Structuring Gold Nanoparticles Using DNA: Towards Smart Nanoassemblies and Facile Biosensors*. PhD Thesis, McMaster University.